Puska, M. J.; Nieminen, R. M.; Manninen, M.

Atoms embedded in an electron gas

Published in:
Physical Review B

DOI:
10.1103/PhysRevB.24.3037

Published: 01/01/1981

Document Version
Publisher's PDF, also known as Version of record

Please cite the original version:
Puska, M. J., Nieminen, R. M., & Manninen, M. (1981). Atoms embedded in an electron gas: Immersion energies. Physical Review B, 24(6), 3037-3047. https://doi.org/10.1103/PhysRevB.24.3037

PHYSICAL REVIEW B VOLUME 24, NUMBER 6 15 SEPTEMBER 1981

Atoms embedded in an electron gas: Immersion energies

M. J. Puska
Department of Technical Physics, Helsinki University of Technology, 02150 Espoo 15, Finland

R. M. Nieminen
Department of Physics, University of Jyväskylä, 40720 Jyväskylä 72, Finland

M. Manninen
NORDITA, Blegdamsvej 17, 2100 Copenhagen, Denmark
(Received 24 March 1981)

Energies of atoms, H through Ar, embedded in a homogeneous electron gas are calculated within the density-functional scheme as a function of the electron-gas density. The energy-versus-density curves and the induced densities of states are analyzed and discussed in terms of the interaction properties of an atom with its environment. The low-density limit of the immersion energy is related to the electron-atom scattering length. The results should prove useful in detailed investigations of the recently suggested "quasiatom" or "effective-medium" approaches to chemical binding. The lowest-order estimates of the binding energies of diatomic molecules and chemisorbed atoms are obtained.

I. INTRODUCTION

A number of properties of inhomogeneous electronic systems have been discussed from the viewpoint of an *atom embedded in an electron gas.* In this approach one generally focuses on a single atom and examines its interaction with a host of extended states using density functional methods. In recent years, models of this type have been investigated in the context of, e.g., chemisorption on metallic surfaces,[1] impurities in bulk metals,[2–5] optical properties of pure metals,[6] interionic forces,[7] etc. While it seems natural that the methods leaning heavily on the existence of a continuum of plane-wave-like states are best suited for systems based on simple metals, their usefulness is by no means limited to them, at least in a qualitative sense. Many of the crucial features of chemical binding that emerge from the continuum-based models hold true also for more complicated systems.

An accurate numerical solution or the problem of an atom interacting with an electron gas can be quite difficult, especially in cases where spatial symmetry is low. Quite recently, Nørskov and Lang,[8] and Stott and Zaremba[9,10] have independently suggested an alternative, simpler way of estimating binding energies of atoms in electronic systems. The central quantity in this "effective-medium" or "quasiatom" approach is the energy change $\Delta E^{\text{hom}}(n_0)$ accompanying the immersion of an atom into a homogeneous electron gas of density n_0. To a first approximation, the actual binding energy ΔE of an atom is then simply given by $\Delta E^{\text{hom}}(\bar{n}_0)$, where $\bar{n}_0$ is some suitably chosen average of the *host* electron density over the region of the atom in question. Systematic corrections can be derived, either in terms of density gradients or response functions describing the unperturbed host system. The approach, based on ideas not too different from those behind the conventional local-density approximations for electronic exchange and correlation, depends on the notion that the electronic structure and total energy of any given (impurity) atom is primarily determined by the immediate local environment in which it immersed. This reflects the tendency to local charge neutrality (screening), which is balanced by energy terms arising from orthogonality and exchange and correlation.

The first applications of the effective-medium or quasiatom theory of chemical binding for hydrogen and oxygen chemisorption on jellium surfaces[8] and for substitutional hydrogen, helium, and lithium impurities in simple metals[9,10] were quite encouraging, and reproduced the qualitative trends of more sophisticated model calculations. It is the purpose of this paper to provide more data bases for this kind

of comparison. In particular, we report $\Delta E^{\rm hom}(n_0)$ curves for atoms in the first three rows of the Periodic Table, and examine the validity of the theory presented in Refs. 8—10 in a number of cases. Our general conclusion corroborates the original arguments: The theory, when properly applied, can be quite useful in achieving the highly desirable goal of determining properties of composite systems from those of their constituents. These, of course, include a vast number of important physical problems ranging from construction of potential-energy surfaces for impurity diffusion to questions of alloy stability. We hope that the data presented here will prove useful in further development of a simpler approach to chemical binding.

The method of calculating $\Delta E^{\rm hom}(n_0)$ is briefly described in Sec. II. Because achieving good numerical convergence and accuracy is central to further developments, the calculation techniques are discussed in some more detail in the Appendix. In Sec. III we give the $\Delta E^{\rm hom}(n_0)$ curves and discuss their systematics. The induced density of states and its angular momentum decomposition are used in further analysis of the trends. We also point out a useful relation between the low-density slope of $\Delta E^{\rm hom}(n_0)$ curve and the scattering length of an electron scattering off a neutral atom. Section IV contains a short discussion, where the results of some simple applications of the effective-medium or quasiatom approach, are compared with exact calculations.

II. ATOMS IN JELLIUM

In the spin-density-functional formalism[11] the ground-state energy of a system of electrons is written as functional of the electron-spin densities $n^s(\vec{r})$ ($s = +$ or $-$):

$$E[n^+,n^-] = T[n^+,n^-] + \frac{1}{2}\int \frac{n(\vec{r})n(\vec{r}')}{|\vec{r}-\vec{r}'|}d\vec{r}\,d\vec{r}' + E_{\rm xc}[n^+,n^-] + \sum_s \int V^s n^s(\vec{r})d\vec{r}\,. \tag{1}$$

Here $n(\vec{r}) = n^+(\vec{r}) + n^-(\vec{r})$ is the total density. $T[n^+,n^-]$ is the kinetic energy of noninteracting electrons and the second term on the right-hand side is the electrostatic Hartree energy of the electrons. $E_{\rm xc}[n^+,n^-]$ is the exchange-correlation energy, and the last term is the energy originating from the interaction with an external potential V^s. In the present case the external potential is due to an (impurity) point charge and a uniform jellium background. The corresponding positive charge is

$$n_+(\vec{r}) = n_0 + Z\delta(\vec{r})\,, \tag{2}$$

where $n_0 = 3/4\pi r_s^3$ is the uniform background density and Z is the nuclear charge of the atom in question.

In the Kohn-Sham method a set of eigenfunctions is solved from the one-electron Schrödinger equations:

$$[-\tfrac{1}{2}\nabla^2 + v^s_{\rm eff}(\vec{r})]\psi^s_i(\vec{r}) = \epsilon^s_i\psi^s_i(\vec{r})\,. \tag{3}$$

The effective spin-dependent potential $v^s_{\rm eff}(\vec{r})$ is

$$v^s_{\rm eff}(\vec{r}) = \phi(\vec{r}) + \frac{\delta E_{\rm xc}[n^+,n^-]}{\delta n^s(\vec{r})}\,, \tag{4}$$

where $\phi(\vec{r})$ is the electrostatic potential of the system, and the last term is the spin-dependent exchange-correlation potential. The spin densities are calculated as sums over occupied orbitals,

$$n^s(\vec{r}) = \sum_i |\psi^s_i(\vec{r})|^2\,. \tag{5}$$

From the spin densities the spin polarization $\zeta(\vec{r})$ is obtained as

$$\zeta(\vec{r}) = [n^+(\vec{r}) - n^-(\vec{r})]/n(\vec{r})\,. \tag{6}$$

The set of equations (3)—(5) is solved self-consistently.

In the local-density approximation the exchange-correlation potential is

$$\frac{\delta E_{\rm xc}[n^+,n^-]}{\delta n^\pm(\vec{r})} = \mu^\pm_{\rm xc} = \epsilon_{\rm xc} + n\frac{\partial\epsilon_{\rm xc}}{\partial n} - (\zeta \mp 1)\frac{\partial\epsilon_{\rm xc}}{\partial\zeta}\,, \tag{7}$$

where $\epsilon_{\rm xc}$ is the exchange-correlation energy per electron in a uniform polarized electron gas of density $n(\vec{r})$ and polarization $\zeta(\vec{r})$. For the exchange-correlation energy we have used the interpolation formula presented by Gunnarsson and Lundqvist.[12] This frequently used interpolation formula does not exactly reproduce the most recent values for the electron gas correlation energy.[13,14] To see the sensitivity of the result to the specific interpolation formula, we calculated the immersion energy $\Delta E^{\rm hom}(n_0)$ (see below) for F, also using a more recent interpolation formula[15] for $\mu_{\rm xc}$. The results for $\Delta E^{\rm hom}$ departed from those calculated using the

Gunnarsson-Lundqvist formula by less than 0.2 eV.

In practice the zero of energy in Eqs. (3)–(5) is defined so that the total effective potential vanishes far away from the atom. In the jellium model this means that the term $\mu_{\rm xc}^s(n_0,\zeta_0)$ has to be subtracted from the potential (4). Here ζ_0 is the polarization of the bulk electron gas. The technique of the iterative solution of Eqs. (3)–(5) is discussed in the Appendix.

If we exclude external magnetic fields, the energy $E^{\rm hom}$ of an atom immersed in an electron gas consists of kinetic, Coulomb, and exchange-correlation terms as

$$E^{\rm hom} = \Delta T + \Delta E_C + \Delta E_{\rm xc} , \tag{8}$$

where the kinetic energy ΔT can be written as

$$\Delta T = \sum_{i,s} \epsilon_i^s + \frac{1}{\pi} \sum_{l,s} \epsilon_F^s (2l+1)\delta_l^s(\epsilon_F^s) - \frac{1}{\pi} \sum_{l,s} \int_0^{\epsilon_F^s} d\epsilon (2l+1)\delta_l^s(\epsilon) - \sum_s \int_0^\infty dr\, 4\pi r^2 v_{\rm eff}^s n^s(r) , \tag{9}$$

where the first term is a sum over the bound states $\epsilon_i^s < 0$ below the bottom of the band, ϵ_F^s is the Fermi kinetic energy for spin s, and δ_l^s is the scattering phase shift. The Friedel sum rule requires that

$$\frac{1}{\pi} \sum_{s,l} (2l+1)\delta_l^s(\epsilon_F^s) = Z . \tag{10}$$

The Coulomb energy is

$$\Delta E_C = \tfrac{1}{2} \int_0^\infty dr\, 4\pi r^2 [n(r) - n_+(r)] \times \left[\phi(r) - \frac{Z}{r} \right] , \tag{11}$$

and the exchange-correlation energy is

$$\Delta E_{\rm xc} = \int_0^\infty dr\, 4\pi r^2 [n(r)\epsilon_{\rm xc}(n(r),\zeta(r)) - n_0 \epsilon_{\rm xc}(n_0,\zeta_0)] . \tag{12}$$

Some numerical points important for an accurate determination of $E^{\rm hom}$ are discussed in the Appendix.

The free-atom energy $E_{\rm atom}$ is obtained via a spin-polarized neutral-atom calculation, using the same exchange-correlation functional. The energy of immersion is defined as the difference

$$\Delta E^{\rm hom}(n_0) = E^{\rm hom}(n_0) - E_{\rm atom} . \tag{13}$$

As shown by Stott and Zaremba,[10] the slope of $\Delta E^{\rm hom}(n_0)$ can be related via the Hellmann-Feynman theorem to the mean Coulomb potential, i.e.,

$$\frac{d\Delta E^{\rm hom}(n_0)}{dn_0} = -\int d\vec{r}\, \phi(\vec{r}) . \tag{14}$$

This relation immediately implies a negative infinite slope at $n_0 = 0$ in cases where the free negative ion is stable, since the integral over the Coulomb potential diverges. On the other hand, Eq. (14) as such does not hold when n_0 is equal to zero; a relation which ties the slope of $\Delta E^{\rm hom}(n_0)$ near the origin to the atomic properties will be discussed in Sec. III.

The atom-induced change in the density-of-spin states $\Delta D^s(\epsilon)$ is also of interest. If we assume that the Kohn-Sham eigenfunctions ψ_i^s give a reasonable description of the one-particle states, a simple formula for $\Delta D^s(\epsilon)$ is obtained. It consists of discrete peaks at the bound-state energies and a continuum part

$$\Delta D^s(\epsilon) = \frac{1}{\pi} \sum_l \frac{\partial \delta_l^s}{\partial \epsilon} (2l+1) . \tag{15}$$

The angular momentum decomposition of $\Delta D(\epsilon)$ can be used in analyzing the various partial-wave contributions to the screening of the embedded atom.

III. RESULTS

The calculated neutral free-atom energies $E_{\rm atom}$ are given in Table I. The calculated energies of immersion $\Delta E^{\rm hom}(n_0)$ are displayed in Figs. 1–4 for elements H through Ar (with the exception of P and S, for which a satisfactory convergence throughout the density range of interest was not achieved). The $n_0 = 0$ intercepts of the curves are drawn to the affinities[16] of the negative ions when stable.

TABLE I. Free-atom energies $E_{\rm atom}$ (eV).

Atom	Energy	Atom	Energy	Atom	Energy
H	−13.3860	N	−1475.98	Al	−6572.23
He	−77.8328	O	−2031.33	Si	−7849.29
Li	−200.887	F	−2700.92	Cl	−12 489.0
Be	−394.538	Ne	−3493.94	Ar	−14 320.3
B	−664.630	Na	−4398.16		
C	−1021.90	Mg	−5424.14		

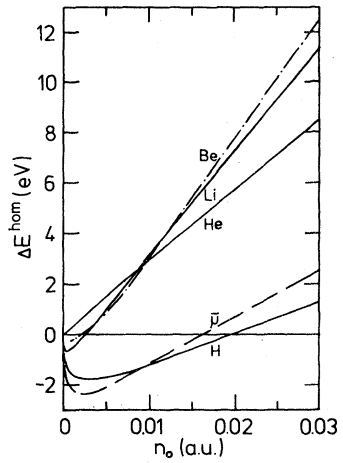

FIG. 1. Immersion energy ΔE^{hom} as a function of electron gas density n_0 for H, He, Li, and Be. $\bar{\mu}$ is the internal chemical potential of the electron gas.

As discussed earlier,[10] the curves $\Delta E^{\text{hom}}(n_0)$ fall into two classes: those with a negative minimum and those without. The former are associated with atoms with stable free negative ions, which implies through Eq. (14) an infinite negative slope at $n_0 = 0$. To the latter belong inert atoms, notably rare gases, and they reflect the basically repulsive interactions of such atoms with any electronic environment. For high enough densities, $\Delta E^{\text{hom}}(n_0)$ for all atoms become positive and approximately linearly rising, which reflects the increasing repulsion connected with the increase in kinetic energy due to orthogonalization or exclusion from the occupied core states. Figure 5 shows the high-density slope (evaluated at $n_0 = 0.03$ or $r_s = 2$) of the $\Delta E^{\text{hom}}(n_0)$ curves as a function of the atomic number Z.

As suggested by Stott and Zaremba,[10] it is instructive to decompose ΔE^{hom} into terms that can be associated with (i) chemical potential effects due

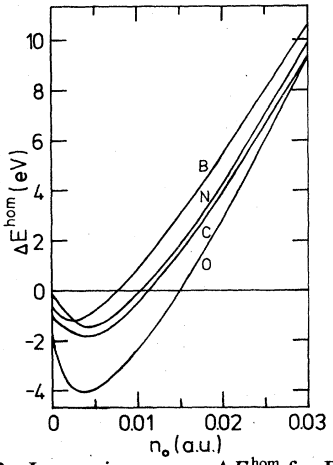

FIG. 2. Immersion energy ΔE^{hom} for B, C, N, and O.

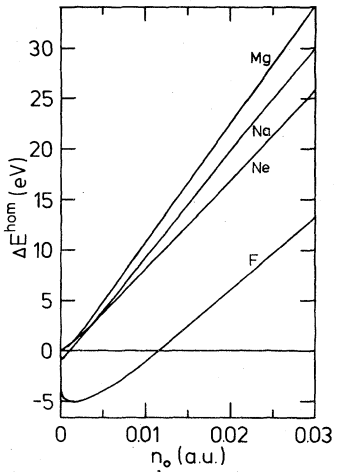

FIG. 3. Immersion energy ΔE^{hom} for F, Ne, Na, and Mg.

to addition of Z electrons on the Fermi level in embedding the (neutral) atoms and (ii) relaxation effects due to improved screening in the metallic environment. That is, ΔE^{hom} is written as

$$\Delta E^{\text{hom}}(n_0) = Z\bar{\mu}(n_0) + \Delta E_R(n_0) , \tag{16}$$

where $\bar{\mu} = \epsilon_F + \mu_{\text{xc}}$ is the internal chemical potential of the electron gas and ΔE_R is (by definition) the relaxation or rearrangement energy. Figure 1 also shows $\bar{\mu}(n_0)$ in the Gunnarsson-Lundqvist[12] approximation. One's prejudice is that at high densities the relaxation energy ΔE_R is only weakly dependent on density [in the extremely-high-density limit RPA gives $\Delta E_R(n_0) \propto n_0^{1/6}$] and will act to compensate the rapid increase ($\propto Z n_0^{2/3}$) in the chemical potential term. This suggests a definition of Z_{eff}, the effective number of electrons in an atom sensitive to environment, as

$$Z_{\text{eff}} = \frac{d\Delta E^{\text{hom}}}{dn_0} \Big/ \frac{d\bar{\mu}}{dn_0} . \tag{17}$$

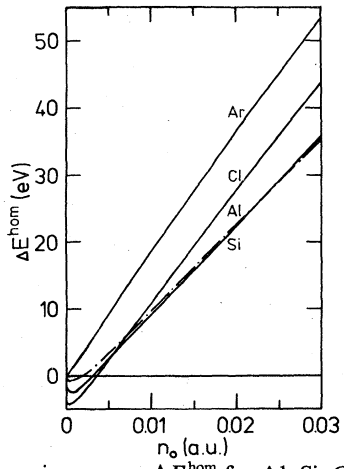

FIG. 4. Immersion energy ΔE^{hom} for Al, Si, Cl, and Ar.

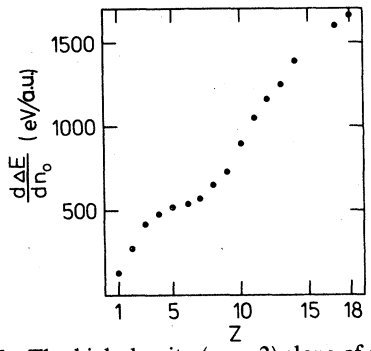

FIG. 5. The high-density ($r_s = 2$) slope of the $\Delta E^{\text{hom}}(n_0)$ curve as a function of the atomic number.

Z_{eff}, evaluated at the linear portion ($n_0 = 0.03$) is given in Table II.

The depths and positions of the minima of the $\Delta E^{\text{hom}}(n_0)$ curves are tabulated in Table III. These are simple but important parameters of the quasiatom description, and we will discuss their applicability to treatment of chemical binding in Sec. IV. In the cases of Li, Be, Na, Mg, and Si where the minimum occurs at a very low density, we were able to estimate accurately only the upper limits for the minimum energies and the corresponding densities.

The curves for H, He, Li, and O have been reported previously. For H, our results agree well with those of Nørskov and Lang[8] and of Stott and Zaremba.[10] For Li our result essentially coincides with that of Stott and Zaremba,[10] and for O the agreement with Ref. 8 is also satisfactory. Differences with Ref. 17 arise, however, in the case of He (Fig. 1). For high densities, the slope of our result (275 eV/a.u.) agrees rather well with Stott and Zaremba[10] but is much less than the value 375 eV/a.u. reported by Esbjerg and Nørskov.[17] In particular, we find no high-slope (≈ 750 eV/a.u.) region for $r_s > 10$, as reported in Ref. 17. For the other two rare gases considered, Ne and Ar, a curve similar to that of He, a monotonously and nearly linearly rising curve, is obtained.

TABLE II. The number of electrons, Z_{eff}, sensitive to the environment as defined by Eq. (17).

Atom	Z_{eff}	Atom	Z_{eff}	Atom	Z_{eff}
H	0.731	N	3.15	Al	6.92
He	1.52	O	3.61	Si	7.66
Li	2.21	F	4.01	Cl	8.81
Be	2.58	Ne	4.98	Ar	9.15
B	2.86	Na	5.43		
C	2.97	Mg	6.39		

TABLE III. Positions ($n_0^{\min}$) and depths of the minima of ΔE^{hom} curves.

Atom	$n_0^{\min}$ (a.u.)	$\Delta E^{\text{hom}}(n_0^{\min})$ (eV)
H	0.0026	-1.8
Li	<0.0010	<-0.6
Be	<0.0005	<-0.2
B	<0.0025	-1.2
C	0.0035	-1.8
N	0.0045	-1.4
O	0.0037	-4.1
F	0.0010	-5.1
Na	<0.0005	<-0.6
Mg	<0.0005	<0.0
Al	0.0005	-0.2
Si	<0.0010	<-1.5
Cl	0.0005	-4.0

The low-density limit of the $\Delta E^{\text{hom}}(n_0)$ curves is interesting. In cases where the negative ion is the correct low-density limit, the integral over the Coulomb potential in Eq. (14) diverges: Thus the curve starts from the affinity value with an infinite negative slope. On the other hand, if the free negative ion is not stable and the correct limit is the neutral atom (e.g., He, Ne, Ar), the slope near the origin may be related to atomic properties as follows.

At a low density, one can view the situation as electrons scattering off a neutral atom. In the limit $n_0 \to 0$, the electron-atom scattering leads to the energy change

$$\Delta E_{e\text{-atom}} = 2\pi a n_0 , \tag{18}$$

where a is the electron-atom scattering length. Equation (18) is the familiar optical potential expression and is valid for any system composed of a particle interacting with scatterers when no bound states exist. The compensating positive background also interacts with the atom, and the corresponding Coulomb energy is

$$\Delta E_b = \int d\vec{r}\,[Z\delta(\vec{r}) - n_{\text{atom}}(\vec{r})]V_b(\vec{r}) , \tag{19}$$

where $n_{\text{atom}}(\vec{r})$ is the atomic electron density and V_b the Coulomb potential due to the background. One finds

$$\Delta E_b = \frac{8\pi^2}{3} n_0 \int_0^\infty dr\, r^4 n_{\text{atom}}(r)$$

$$= -4\pi n_0 \int_0^\infty dr\, r^2 \phi_{\text{atom}}(r) , \tag{20}$$

where ϕ_{atom} is the Coulomb potential of the atom. The total energy of immersion is in the low-density limit

$$\Delta E^{\text{hom}} \xrightarrow[n_0 \to 0]{} \Delta E_{e\text{-atom}} + \Delta E_b \ . \tag{21}$$

Combining Eqs. (18) and (20), we find

$$\frac{d\Delta E^{\text{hom}}}{dn_0}\underset{n_0 \to 0}{=} 2\pi a - \int d\vec{r}\,\phi_{\text{atom}}(r) = 2\pi a + \frac{8\pi^2}{3}\int_0^\infty dr\, r^4 n_{\text{atom}}(r) \ . \tag{22}$$

Note that the limiting form (22) cannot be obtained from relation (14) by substituting ϕ by ϕ_{atom}. The reason is that in the derivation of Eq. (14) the derivative $d\bar{\mu}/dn_0$ is needed; this diverges as $n_0^{-2/3}$ at low densities. The scattering length a is *not* directly related to the phase shifts of an electron scattering off the self-consistent atom potential. It should be calculated from a self-consistent potential including the scattering electron itself, as done implicitly in the above derivation.

Equation (22) is exact and thus provides a way to calculate the zero-energy scattering length once $d\Delta E/dn_0$ near $n_0 = 0$ and ϕ_{atom} (or n_{atom}) are known. In the present work, those are obtained within the local-density approximation for exchange and correlation. Table IV lists the calculated scattering lengths for He, Ne, and Ar atoms; the experimental estimates due to O'Malley[18] are also included. The agreement is quite satisfactory for He and Ne, but less so for Ar. Note, however, that the value of a is very sensitive to the large-r behavior of the atomic electron density $n_{\text{atom}}(r)$. Within the local-density approximation, the effective potential decays exponentially for large distances, whereas the true potential is proportional to $-r^{-1}$. Thus, improving on the local-density approximation would slightly relax $n_{\text{atom}}(r)$ outwards, making $\int dr\, r^4 n_{\text{atom}}(r)$ larger and consequently *diminish* a.

TABLE IV. The scattering lengths a (in atomic units) of the rare-gas atoms as calculated from Eq. (22). The experimental estimates are from Ref. 18.

Atom	a [Eq. (22)]	a_{expt}
He	0.932	1.12—1.19
Ne	0.63	0.14—0.39
Ar	1.52	−1.4— −1.70

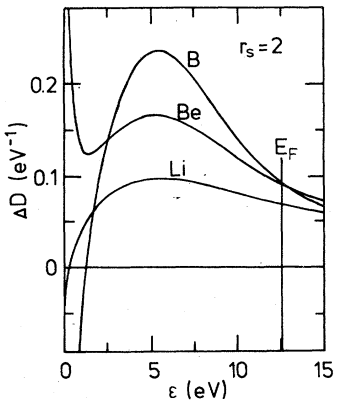

FIG. 6. Induced state densities $\Delta D(\epsilon)$ for Li, Be, and B in the case $r_s = 2$.

This would presumably yield better agreement in the case of Ar. It would be very interesting to test corrections to the local-density approximation (such as self-interaction corrections,[6,19] sampling function schemes,[20] gradient expansions[21]) by calculating the zero-energy atomic scattering lengths from Eq. (22).

Examples of the continuum part of the induced density of state $\Delta D(\epsilon)$ are shown in Figs. 6—11. Figures 6 and 7 display the induced state density for atoms Li through F, for the case $r_s = 2$. Figures 8 and 9 exhibit the partial-wave decompositions of $\Delta D(\epsilon)$ for Li, C, Ne, Na, Si, and Ar. As $\epsilon \to 0$, $\Delta D(\epsilon)$ has a weak singularity which is due to s-wave scattering. This divergence can be either positive or negative [see Figs. (8)—(11)]. The change of sign of low-energy divergence in the s-wave contribution to the induced density of states can simply be understood, by way of an example, by considering scattering off a square well of radius b and depth $V_0 = k_0^2/2$. The s-wave phase shift is

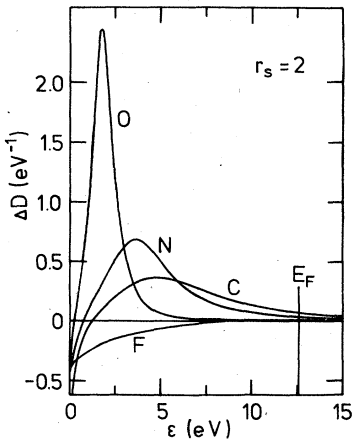

FIG. 7. Induced state densities $\Delta D(\epsilon)$ for C, N, O, and F in the case $r_s = 2$.

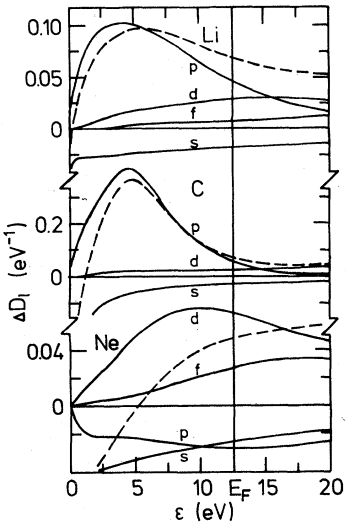

FIG. 8. Partial-wave decompositions of $\Delta D(\epsilon)$ for Li, C, and Ne in the case $r_s = 2$. The dashed curves give the total induced density of states.

$$\delta_0(k) = \arctan\left[\frac{k}{(k_0^2 + k^2)^{1/2}}\tan(k_0^2 + k^2)^{1/2}a\right] - ka + n\pi\,, \tag{23}$$

where n is the number of bound states in the well. The induced state density in the limit $\epsilon \to 0$ is

$$\Delta D_0(\epsilon) = (\tan k_0 a - k_0 a)\sqrt{2}/\pi k_0\sqrt{\epsilon}\,. \tag{24}$$

Thus there is a divergence proportional to $\epsilon^{-1/2}$, the sign of which changes as a function of the well parameters. The low-energy divergence is positive for $k_0 a < \pi/2$ (when there is no bound state) and

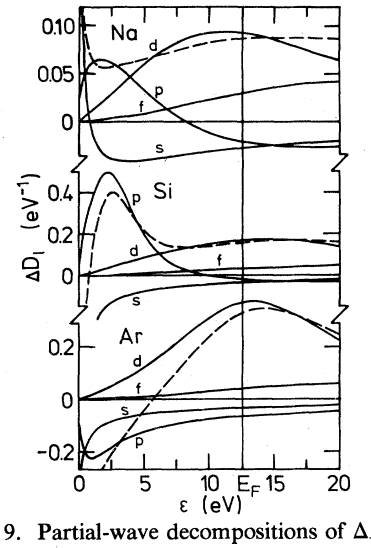

FIG. 9. Partial-wave decompositions of $\Delta D(\epsilon)$ for Na, Si, and Ar in the case $r_s = 2$. The dashed curves give the total induced density of states.

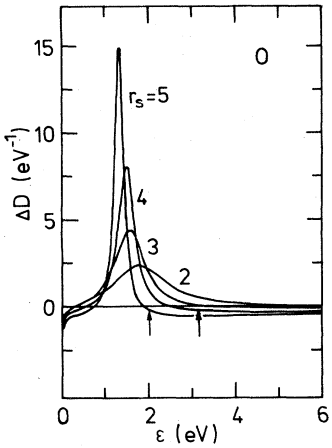

FIG. 10. The induced state density $\Delta D(\epsilon)$ for O at different densities n_0. The arrows denote the position of the Fermi level in each case.

before the appearance of successive new bound states in regions between the roots of equation $\tan k_0 a = k_0 a$ and odd multiples of $\pi/2$. The divergence is negative after the appearance of a new bound state. Similar divergence with an alternating sign in the s-wave density of states holds for any potential decaying faster than r^{-2}.

As noted by Stott and Zaremba, p-wave scattering is already substantial for Li (Fig. 8); for the other second-row elements p-wave character increases with Z and is totally dominating in C, N, and O. For F the $2p$ electrons are bound at $r_s = 2$ and the conduction-band contribution to $\Delta D(\epsilon)$ consequently changes drastically. It has a strong d-like character, which is even more pronounced for Ne. In the following row (Fig. 9), Na and Mg have nearly flat induced state densities when $r_s = 2$, whereas Al and especially Si have p-like peaks. Cl binds the $3p$

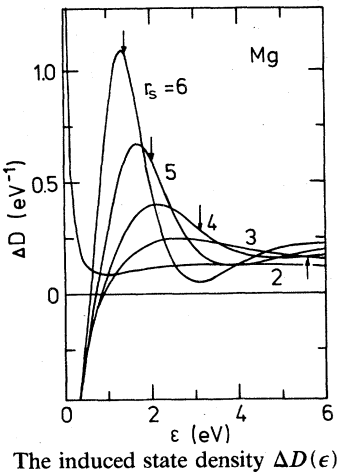

FIG. 11. The induced state density $\Delta D(\epsilon)$ for Mg at different densities n_0. The arrows denote the position of the Fermi level in each case.

electrons and, not surprisingly, shows structure resembling F.

The dependence of the induced state density on the jellium density is displayed in Figs. 10 and 11 for O and Mg, respectively. The figures show the formation and movement of a p-like resonance within the Fermi sea. It is also noteworthy that Mg binds the $3s$ electrons when $r_s > 3$ and therefore the $\epsilon^{-1/2}$ singularity changes sign when going from $r_s = 2$ to $r_s = 3$. One can also note, especially in the case of O, that the peak in the induced density of states is rather fixed in energy and does not follow the Fermi level.

IV. DISCUSSION

The quasiatom or effective-medium approach to chemical binding is appealing. In its simplest form, the uniform density approximation, the ansatz simply states that the binding energy E_B of an atom to any inhomogeneous electronic medium is given by

$$E_B = \Delta E^{\text{hom}}(n(\vec{r}=0)) , \tag{25}$$

where $n(\vec{r}=0)$ is the host electron density at the site where the (impurity) atom nucleus is placed. A useful improvement is to use instead of the local density the effective "sampled" density around the nucleus. If the sampling function is chosen to be the induced Coulomb potential in a homogeneous medium, the leading correction to E_B reduces to the simple first-order electrostatic energy.[8,10] Further corrections can be systematically obtained, e.g., in terms of density-density response functions for the embedded atom.

Detailed investigations of various systems will be necessary to reveal the general applicability, convergence, and accuracy of the quasiatom approach. Here we restrict ourselves to some simple and general observations. Table V lists the average binding energies of those diatomic molecules, where one of the atom belongs to the group considered in Sec. III. Also, the mean-square deviations are listed. Two entries are given for each atom: The first entry includes all diatomic binding energies tabulated in Ref. 22; the second, labeled "metallic," includes only those where the second atom belongs to the metallic elements of the Periodic Table. Upon comparison with the minimum ΔE^{hom} energies of Table II, one notes that the correlation is certainly suggestive, especially when the atom in question either forms a good metal or is strongly electronegative. On the other hand, the correlation seems to be quite poor in cases where the atom is known to have the tendency to bond covalently. Whether effects like covalency can be incorporated in, say, corrections to the uniform-density approximation, remains an interesting question worth investigating.

A straightforward test case, already considered in Refs. 8 and 10, is atomic chemisorption on simple metal (jellium) surfaces. This problem has been investigated in detail using density-functional methods, and the results[1] for the binding energy and equilibrium distance from the jellium edge are collected in

TABLE V. Average experimental bond strengths and their standard deviations for diatomic molecules. The right-hand column includes only molecules with a metallic partner. The number of molecules is given in parentheses. Data from Ref. 22.

Atom	$\bar{E}_B$ (eV)	$\bar{E}_B$ ("metallic")
H	-2.7 ± 1.0 ($n = 43$)	-2.2 ± 0.7 ($n = 26$)
Li	-3.9 ± 1.5 ($n = 6$)	-1.0 (Li_2)
Be	-3.6 ± 1.5 ($n = 6$)	-0.7 (Be_2)
B	-4.8 ± 1.5 ($n = 17$)	-4.3 ± 0.8 ($n = 8$)
C	-5.8 ± 1.8 ($n = 20$)	-5.9 ± 0.6 ($n = 7$)
N	-4.6 ± 1.9 ($n = 17$)	-4.8 ± 1.1 ($n = 4$)
O	-5.1 ± 1.8 ($n = 70$)	-4.3 ± 1.5 ($n = 20$)
F	-4.8 ± 1.3 ($n = 32$)	-4.9 ± 0.9 ($n = 17$)
Na	-2.2 ± 1.5 ($n = 6$)	-0.7 ± 0.1 (Na_2,NaRb)
Mg	-2.5 ± 1.0 ($n = 6$)	-1.5 ± 1.1 ($n = 3$)
Si	-4.1 ± 1.0 ($n = 16$)	-3.6 ± 0.8 ($n = 9$)
Cl	-3.4 ± 0.9 ($n = 33$)	-3.7 ± 0.6 ($n = 23$)

Table VI. The final entries in the table are the simple uniform-density-approximation estimates for those numbers. These can easily be read from the curves of Sec. III once the density profile for the pure jellium surface[23] is at hand. Again we notice a good overall agreement, which gives support to the basic soundness of the quasiatom concept. (Also the form of potential energy curves near the chemisorption minimum is rather well reproduced.)

One immediate application of the quasiatom approach is the construction of an effective interatomic potential. In the region where the $\Delta E^{\text{hom}}(n_0)$ curve is linearly rising with density, the interaction energy of an atom with its environment is a linear function of the density. If the total density is imagined to be constructed as a superposition of (pseudo)atomic charge densities, the linearity of $\Delta E^{\text{hom}}(n_0)$ implies that the total energy of interaction of an atom with the surrounding ones is also obtained as superposition of interaction energies, i.e., there is a well-defined interatomic *pair* potential. This idea may turn out quite useful in obtaining potential-energy surfaces, and indeed Esbjerg and Nørskov[17] have analyzed He scattering from metal surfaces in these terms.

In conclusion, energies of immersion of atoms H through Ar in a homogeneous electron gas have been obtained in the density range $r_s = 2-8$ using a self-consistent solution of density-functional equations. These energies contain useful information about the binding characteristics of atoms in a form which promises to be most useful in a number of applications. Further work will be necessary to investigate the accuracy of a perturbative approach to

TABLE VI. Chemisorption energies and distances for atoms on jellium surfaces, evaluated in the uniform density approximation using density profiles from Ref. 23, and Figs. 1–4. The right-hand columns for $r_s = 2$ are the exact results of Lang and Williams (Ref. 1).

$r_s = 2$	Uniform density approximation		Lang and Williams (Ref. 1)	
Atom	Energy (eV)	Distance (a.u.)	Energy (eV)	Distance (a.u.)
H	−1.8	1.6	−1.5	1.1
Li	< −0.6	> 2.3	−1.3	2.5
Be	< −0.2	> 3.0		
B	−1.2	1.6		
C	−1.8	1.3		
N	−1.4	1.1		
O	−4.1	1.3	−5.4	1.1
F	−5.1	2.3		
Na	< −0.6	> 3.0	−0.9	3.1
Mg	< 0.0	> 3.0		
Al	−0.2	3.0		
Si	< −1.5	> 2.3	−3	2.3
Cl	−4.0	3.0	−3.6	2.6

$r_s = 4$	Uniform density approximation	
Atom	Energy (eV)	Distance (a.u.)
H	−1.8	−1.1
Li	< −0.6	> 0.6
Be	< −0.2	> 1.5
B	−1.2	−1.0
C	−1.8	−2.1
F	−5.1	0.6
Na	< −0.6	> 1.5
Mg	< 0.0	> 1.5
Al	−0.2	1.5
Si	< −2.5	> 0.6
Cl	−4.0	1.5

chemical bonding based on the quasiatom or effective medium concept.

APPENDIX: NUMERICAL TECHNIQUES

Iteration

The iterative solution of Eqs. (3)–(5) has been obtained using the technique of Manninen *et al.*[24] The r axis was discretized into a Herman-Skillmann[25] mesh consisting of 11 blocks, each divided in to 40 intervals. In the free-atom and ion calculations the step length in the first block was taken as

$$\Delta r = 0.00125(3\pi/4)^{2/3}Z^{-1/3} . \quad \text{(A1)}$$

In the jellium calculations, the step lengths were shortened to make the interval in the outermost block small compared to the wavelength π/k_F of the Friedel oscillations. This was accomplished by choosing the largest r-value R_0 to be approximately five times r_s. Beyond this point the scattering state solutions were fitted to their asymptotic forms

$$[\cos\delta_l(k)j_l(kr) - \sin\delta_l(k)n_l(kr)] .$$

Partial waves up to $l = 10$ were included. The $\vec{k}$-space integrals were performed using Simpson's rule on a mesh consisting of up to 61 equally spaced points from 0 to k_F. As the starting potential we have found it convenient to use the Thomas-Fermi potential of the free atom as given by the interpolation formula due to Latter.[26]

In some cases a very shallow bound state appears below the bottom of the band, or a pronounced resonance may develop near the Fermi level. Then, in addition to the inherent stability afforded by the screened-kernel iteration of the Hartree potential, special care is necessary in order to obtain true convergence. For example, the resonance in the conduction band may move across the Fermi level in successive iterations and cause large fluctuations in the screening cloud and thus in the effective potential. A commonly used method to improve stability is to feed into an iteration a linear combination of the initial and final potential from the previous iteration:

$$V_{\text{eff}}^{(m+1)i}(r) = [1 - A(r)]V_{\text{eff}}^{mi}(r) + A(r)V_{\text{eff}}^{mf}(r) , \quad \text{(A2)}$$

where $V_{\text{eff}}^{mi}(r)$, $V_{\text{eff}}^{mf}(r)$ are the intial and final potentials of the mth iteration, and $A(r)$ is a feedback function. The simplest choice is to use a constant $A(r)$.

In the Pratt[27] improvement scheme the initial potential of the next iteration is calculated from initial and final potentials of two latest iterations:

$$V_{\text{eff}}^{(m+1)i}(r) = \frac{V_{\text{eff}}^{(m-1)i}(r)V_{\text{eff}}^{mf}(r) - V_{\text{eff}}^{mi}(r)V_{\text{eff}}^{(m-1)f}(r)}{V_{\text{eff}}^{(m-1)i}(r) + V_{\text{eff}}^{mf}(r) - V_{\text{eff}}^{mi}(r) - V_{\text{eff}}^{(m-1)f}(r)} . \quad \text{(A3)}$$

This means that one attempts to find the self-consistent potential (which satisfies $V_{\text{eff}}^{mi} = V_{\text{eff}}^{\text{mf}}$) by interpolating or extrapolating from the points $(V_{\text{eff}}^{mi}(r), V_{\text{eff}}^{mf}(r))$ and $(V_{\text{eff}}^{(m-1)i}(r), V_{\text{eff}}^{(m-1)f}(r))$ to the line $V_{\text{eff}}^{i}(r) = V_{\text{eff}}^{f}(r)$.

The feedback function $A(r)$ of Pratt's scheme can be solved from Eqs. (A2) and (A3). In the modified Pratt's scheme, which we have used, only the values between 0 and 1 are allowed to $A(r)$. If the calculated $A(r) > 1$ it is replaced by 1. If $A(r) < 0$ it is replaced by a suitably chosen constant. Our method differs slightly from the modified Pratt's scheme used by Herman and Skillmann[25]: They allowed $A(r)$ to vary only between 0.5 and 1. This difference is important because in some cases (see below) the feedback function has to be as small as 0.1–0.2 in order to ensure convergence.

The modified Pratt improvement scheme turns out to be powerful when there is a resonance in the density of states near the Fermi level. Examples of this kind of system are $3d$ impurities in aluminum[5] and C, N, and O atoms in jellium. The origin of the resonance is in the former case resonant d-wave, and in the latter case resonant p-wave scattering. In these systems the Pratt improvement scheme makes the iteration process converge faster than the use of a constant feedback parameter, because in Pratt's scheme $A(r)$ is in these cases a decreasing function of r. Far away from the impurity, where the contribution from the resonance to the total electron density is dominant, the feedback function $A(r)$ is small, which increases stability. In systems where the resonance is near the bottom of the conduction band (e.g., C, N, and O atoms in low-density jellium), the iteration process did not converge even if we used the Pratt scheme. In those cases the resonant electrons in successive iterations sometimes bind and sometimes form a resonance peak above the band bottom. When there is no resonance the iteration process converges rapidly by simply using a constant feedback function $A(r)$, and the Pratt improvement scheme is necessary only in the resonance cases.

Evaluation of total energy

In the $\vec{r}$-space integrals in Eqs. (9), (11), and (12) the limit $r = \infty$ has to be replaced in numerical calculations by the cutoff radius R_0 of the integration mesh. This cutting leads to an R_0 dependence in the calculated total energy. The dependence is largest in the exchange-correlation energy. The integrals in the Coulomb and kinetic energies depend only weakly on R_0, because in the integrands two oscillating functions, charge or spin density and potential, are multiplied. We have removed the R_0 dependence in the exchange-correlation energy by evaluating the correction term (which is valid when $\zeta_0 = 0$)

$$\left[\epsilon_{xc}(n_0,0) + n_0 \frac{d\epsilon_{xc}(n,0)}{dn}\bigg|_{n=n_0}\right]\left[Z - \int_0^{R_0}[n(r) - n_0]4\pi r^2 dr\right] = \mu_{xc}(n_0,0)\left[Z - \int_0^{R_0}[n(r) - n_0]4\pi r^2 dr\right]. \tag{A4}$$

The correction (A4) is the leading term when the exchange-correlation energy density $\epsilon_{xc}(n,0)$ is expanded in a series around n_0 and the integral is calculated analytically from R_0 to infinity.

[1]See, e.g., N. D. Lang and A. R. Williams, Phys. Rev. B 18, 616 (1978), and references therein; H. Hjelmberg, O. Gunnarsson, and B. I. Lundqvist, Surf. Sci. 68, 158 (1977), and references therein. For a recent review, see N. D. Lang, in *Theory of the Inhomogeneous Electron Gas,* edited by S. Lundqvist and N. H. March (Plenum, New York, 1981).

[2]Z. D. Popovic and M. J. Stott, Phys. Rev. Lett. 33, 1164 (1974).

[3]M. Manninen, P. Hautojärvi, and R. Nieminen, Solid State Commun. 23, 795 (1977).

[4]J. K. Nørskov, Phys. Rev. B 20, 446 (1979).

[5]R. M. Nieminen and M. J. Puska, J. Phys. F 10, L123 (1980).

[6]G. W. Bryant and G. D. Mahan, Phys. Rev. B 17, 1744 (1978); G. W. Bryant, Phys. Rev. B 19, 2801 (1979); 19, 2864 (1979).

[7]M. Manninen, P. Jena, R. M. Nieminen, and J. K. Lee, Phys. Rev. B, in press.

[8]J. K. Nørskov and N. D. Lang, Phys. Rev. B 21, 2131 (1980).

[9]M. J. Stott and E. Zaremba, Solid State Commun. 32, 1297 (1979).

[10]M. J. Stott and E. Zaremba, Phys. Rev. B 22, 1564 (1980).

[11]W. Kohn and L. J. Sham, Phys. Rev. 140, A1133 (1965); U. von Barth and L. Hedin, J. Phys. C 5, 1629 (1972).

[12]O. Gunnarsson and B. I. Lundqvist, Phys. Rev. B 13, 4274 (1976).

[13]D. Ceperley, Phys. Rev. B 18, 3126 (1978).

[14]L. J. Lantto, Phys. Rev. B 22, 1380 (1980).

[15]S. H. Vosko, L. Wilk, and M. Nusair, Can. J. Phys. 58, 1200 (1980).

[16]H. Hotop and W. C. Lineberger, J. Phys. Chem. Ref. Data 4, 539 (1975).

[17]N. Esbjerg and J. K. Nørskov, Phys. Rev. Lett. 45, 807 (1980).

[18]T. F. O'Malley, Phys. Rev. 130, 1020 (1963).

[19]A. Zunger, J. P. Perdew, and G. L. Oliver, Solid State Commun. 34, 933 (1980).

[20]O. Gunnarsson, M. Jonson, and B. I. Lundqvist, Phys. Rev. B. 20, 3136 (1979).

[21]F. Herman, J. P. van Dyke, and I. B. Ortenburger, Phys. Rev. Lett. 22, 807 (1969).

[22]J. A. Kerr, M. J. Parsonage, and A. F. Trotman-Dickenson, in *Handbook of Chemistry and Physics,* edited by R. C. Weast (CRC, Ohio, 1975), p. F-204.

[23]N. D. Lang and W. Kohn, Phys. Rev. B 1, 4555 (1970).

[24]M. Manninen, R. Nieminen, P. Hautojärvi, and J. Arponen, Phys. Rev. B 12, 4012 (1975).

[25]F. Herman and S. Skillman, *Atomic Structure Calculations* (Prentice-Hall, Englewood Cliffs, 1963).

[26]F. Latter, Phys. Rev. 99, 510 (1955).

[27]G. Pratt, Phys. Rev. 88, 1217 (1953).